Available online at www.sciencedirect.com
ScienceDirect
Marine Chemistry 102 (2006) 159–169
MARINE CHEMISTRY
www.elsevier.com/locate/marchem

Oxygen depletion in the upper reach of the Pearl River estuary during a winter drought

Minhan Dai [a,*], Xianghui Guo [a], Weidong Zhai [a], Liangying Yuan [a], Bengwang Wang [a], Lifang Wang [a], Pinghe Cai [a], Tiantian Tang [a], Wei-Jun Cai [b]

[a] State Key Laboratory of Marine Environmental Science, Xiamen University, Xiamen 361005, China
[b] Department of Marine Sciences, the University of Georgia, Athens, Georgia 30602, USA

Accepted 8 September 2005
Available online 24 January 2006

Abstract

We examined dissolved oxygen (DO), the carbonate system and nutrients in the upper reach of the Pearl River estuary in a very dry season in February of 2004. We observed very low DO, down to <12–30 μmol O_2 kg^{-1} in the surface water, upstream of the vicinity of the Humen outlet, one of the major water channels into the estuary. The oxygen depleted water body encompasses a surface area of >20 km^2 within a salinity range between 1 and ~5. Accompanied with the low DO were extremely high pCO_2 (up to >7000 μatm) and nutrients (ammonia >600 μmol kg^{-1} and nitrate >200 μmol kg^{-1}). In addition to the aerobic respiration, processes such as nitrification substantially contributed to the consumption of DO, and may have a significant impact on the distribution pattern of the carbonate species including pH. Oxygen depletion was also observed in this area during our prior cruises in other seasons, signifying an alarming environmental condition in the region.

1. Introduction

A water body that has a dissolved oxygen (DO) level below ~90 μmol O_2 kg^{-1} (or 3 mg L^{-1}) is commonly termed as being "hypoxic". There have been numerous reports of low dissolved oxygen or oxygen depletion in the world coastal environment since the last decade (Engle et al., 1999; Abril et al., 2000; Abril and Frankignoulle, 2001; Rabalais and Turner, 2001; Li et al., 2002; Rabalais et al., 2002). For example, a large area of bottom oxygen depletion has been documented in the Yangtze River plume (Li et al., 2002). Shelf waters in the Gulf of Mexico have even become a so-called "dead-zone" with DO below 60 μmol O_2 kg^{-1} (Engle et al., 1999; Ritter and Montagna, 1999; Rabalais et al., 2002). Some European estuaries, such as Forth, Scheldt, Seine, Lorire, are also oxygen depleted to different degrees, largely attributable to anthropogenic discharges (Abril et al., 2003; Abril and Frankignoulle, 2001; Balls et al., 1996; Frankignoulle et al., 1996; Garnier et al., 2001; Hellings et al., 2001).

Most hypoxic cases thus far have been found in bottom waters in either salt wedge estuaries or on coastal shelves during stratifying seasons, typically in late spring and/or summer (Kemp et al., 1992; Ritter and Montagna, 1999). This bottom oxygen depletion

* Corresponding author. Environmental Science Research Center, Xiamen University, Xiamen 361005, China. Tel.: +86 592 2182132; fax: +86 592 2180655.
E-mail address: mdai@xmu.edu.cn (M. Dai).

0304-4203/$ - see front matter © 2006 Elsevier B.V. All rights reserved.
doi:10.1016/j.marchem.2005.09.020

generally results from a combination of eutrophication-induced high biological productivity and restricted water exchange (Borsuk et al., 2001; Kemp et al., 1992; Lawrence et al., 1990). We report in this paper a case of hypoxia expanded in the surface water located at the upper reach of the Pearl River estuary. Special effort is given here to examine the processes associated with this oxygen depletion, including nitrification that apparently contributes much to the oxygen consumption, and its linkage with the aquatic carbonate system. Similar low DO in surface waters has been observed in European estuaries such as the Forth and Scheldt River Estuaries (Balls et al., 1996; Frankignoulle et al., 1996; Frankignoulle et al., 1998; De Bie et al., 2002; Hellings et al., 2001), but direct linkages between oxygen consumption and the aquatic carbonate system have not been emphasized in these prior researches. Reports have been especially rare for Asian large river estuarine systems such as the Pearl River estuary; these systems have been experiencing extremely rapid changes caused by anthropogenic input during the last two decades.

2. Materials and methods

2.1. Study area

The Pearl River is the largest river in southern China and ranks 13th in the world in terms of freshwater discharge. Its drainage basin is located in a sub-tropical climate zone with annual rainfall of 1600–2300 mm (Huang et al., 2003). The annual water discharge of the Pearl River is ~3.26×10^{11} m^3, 80% of which takes place in the wet season from April to September (Zhao, 1990).

The Pearl River has three major tributaries (Fig. 1), namely Xijiang (West River), Beijiang (North River) and Dongjiang (East River), as well as many netlike small tributaries. All runoff of the tributaries discharge into the South China Sea (SCS) via eight major outlets (PRWRC/PRRCC, 1991), among which, Humen is the largest outlet of the four eastern outlets (Fig. 1) and is a strong-tidal outlet with anomalous semi-diurnal tides. The tidewater through Humen is responsible for ~60 % of the tidewater among all of the eight outlets (Cheng, 2001).

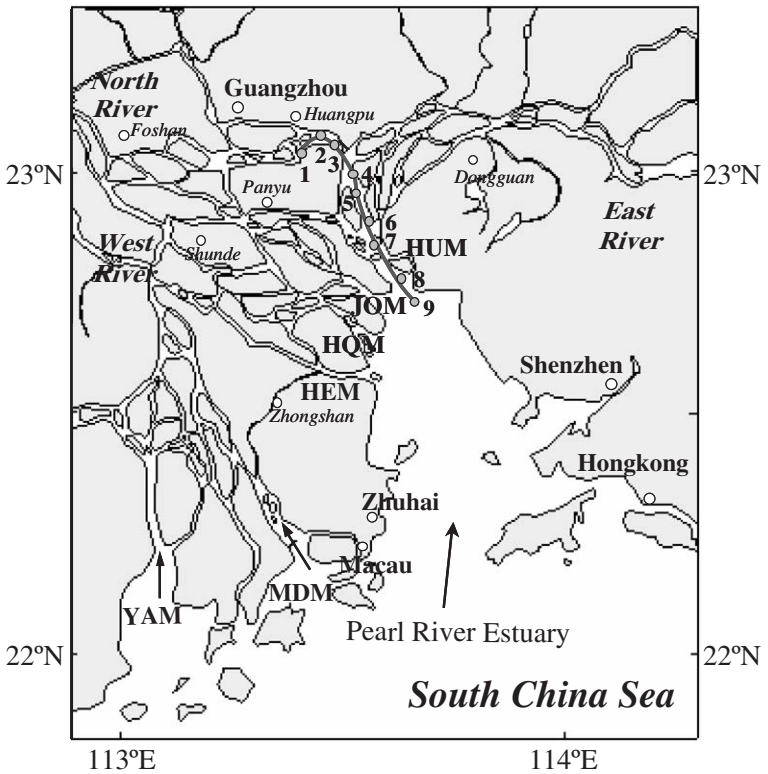

Fig. 1. Map of the Pearl River estuary and sampling stations along with the cruise tracks. We cruised upstream from Sta. 9, the Humen Outlet to Sta. 1, the Huangpu district of Guangzhou and then cruised back to the Humen Outlet. HUM, JOM, HQM and HEM designate Humen, Jiaomen, Hongqimen, and Hengmen representing the eastern four outlets of the Pearl River estuary.

This study considers only the upper reach of the Pearl River estuary from the Humen outlet upward to the suburb of Guangzhou (Huangpu, Fig. 1). This section of the estuary is ~50 km long with an average width of ~2.2 km and an average water depth of 6.6 m (Guangzhou Chorography Compilation Committee, 1998). It receives most of the waste water and sewage discharged from Guangzhou, a metropolis of southern China with a population of >10 million. Among others, two major highly industrialized cities of Guangdong province located along this section of the estuary are Foshan and Dongguan. As a consequence of the waste discharge characterized with heavy organic loads (Tao and Hills, 1999; Table 1), the aquatic environment of the Pearl River/estuary has been deteriorated dramatically in recent years. Average DO of the Guangzhou reach of the Pearl River declined from 113 μmol O_2 kg^{-1} in 1990 to 75 μmol O_2 kg^{-1} in 1998 (Zhang et al., 1999).

It should be noted that the focal area of this study is much different in many ways from the typical estuarine mixing zone of the Pearl River estuary given that the sampling period of Feb 2004 represented an extreme drought and low-flow condition (http://www.fswater.gov.cn). Rain precipitations at Guangzhou between Oct 2003 and Feb 2004 were merely 153 mm (summarized based on http://ccar.ust.hk/dataview/stnplot/current/), representing only ~60 % of the long term average. Numerous hydrological observatories documented a historically low water table and runoff during this period of time (http://www.fswater.gov.cn). As a consequence, the salinity at the vicinity of the Humen Outlet was ~17 during our Feb 2004 sampling period as opposed to ~0 during typical summer and spring seasons, as documented by Cai et al. (2004) and Zhai et al. (2005). In this context, we are looking at a zone of estuarine mixing with prolonged water residence time due to the low river flow.

2.2. Sampling

The study area is shown in Fig. 1. Data were collected in Feb 2004 on board the R/V Yanping II. We cruised upstream (upstream survey hereafter) from Sta. 9, the Humen Outlet to Sta. 1, the Huangpu district of Guangzhou during a neap tide period and then cruised back to the Humen Outlet (downstream survey hereafter) (Fig. 1) during the following flood tide.

Underway pumping was performed for continuous measurements of temperature, salinity, dissolved oxygen (DO), pH and partial pressure of CO_2 (pCO_2). Discrete underway sampling was also conducted for DIC (Dissolved Inorganic Carbon), TAlk (Total Alkalinity), nutrients and DO/pH calibration via a side vent of the DO-pCO_2 pumping system. During the downstream survey, in addition to the underway measurements, we sampled at 9 stations with salinity gradients from the upper most Sta. 1 to Sta. 9, the latter is located just downstream to the Humen Outlet. Vertical profiles of the water column were sampled at 4 selected stations.

Table 1
Quantity of wastewater discharge from Guangdong Province, China between 1990 and 2003

	1990[a]	1995[a]	1996[a]	1997[a]	1998[b]	1999[b]	2000[b]	2001[b]	2002[b]	2003[b]
Total volume of wastewater discharged (10^6 tons)	2512	3816.5	3714	4198	4341	4287	4475	5114	4904	5464
Domestic sewage (% of total discharge)	44	56	57	70	73	73	75	78	70	73
Industrial effluent (% of total discharge)	56	44	43	30	27	27	25	22	30	27
Total volume of chemical oxygen demand (COD) emission in wastewater (10^6 tons)	0.695	1.12	1.06	0.95	0.36	0.34	0.28	0.216	0.207	0.211
Overall rate of domestic sewage treatment (%)	–	–	–	9.0	–	–	–	–	–	35
Overall rate of industrial wastewater treatment (%)	56.8	77.1	80.2	85.3	89.2	–	96.2	96.2	–	–
Overall rate of industrial wastewater recovered (%)	–	43.4	49.8	45.0		89.9	–	–	–	–
Rate of industrial wastewater meeting discharge standard (%)	47.1	56.3	57.7	56.7	61.6	64.9	81.8	81.8	78.3	82.9
Capacity of domestic sewage treatment (10^6 tons)	–	–	–	–	511	–	–	–	–	1455

Also included are the percentage of domestic sewage and waste treatment rate in the total discharged waste.
[a] From Ho and Hui (2001).
[b] Based on Environmental Status Bulletins of Guangdong Province, China at http://www.gdepb.gov.cn/.

2.3. Analysis

2.3.1. Temperature, salinity and meteorological data

Surface temperature and salinity were measured continuously using a SEACAT CTD system (SBE21, Sea-Bird Co.) with an in situ temperature sensor. Data were recorded every 6 s and averaged to 1 min. Vertical profiles of temperature and salinity were obtained with another SEACAT CTD system (SBE19, Sea-Bird Co.), with which data were recorded every 0.5 s. Meteorological data including wind speed were collected with an onboard weather station at ~10 m height above sea surface.

2.3.2. Surface DO, pH and pCO_2

Surface water DO and pH were continuously determined using a Yellow Springs Instrument meter (YSI 6600), which was combined with a continuous flow equilibrator for our pCO_2 measurement. Detailed configuration of our underway measurement system has been given in Zhai et al. (2005). Precisions of the YSI probes were 0.3 μmol kg^{-1} for DO and 0.01 units for pH. The DO probe was pre-calibrated with water saturated air, and the pH probe was pre-calibrated using NBS (now NIST)-traceable pH buffers. DO probe data were also calibrated against Winkler DO data using discrete water samples. The DO concentrations determined with the two methods agreed very well with each other, the average difference of which was 3.4 μmol O_2 kg^{-1}.

pCO_2 was determined using a system that combined a Li-Cor® non-dispersive infrared (NDIR) spectrometer with a continuous flow equilibrator, as detailed in Zhai et al. (2005). In this study we used a LI-7000, which has a broader linear response range than the Li-Cor 6252 or 6262 that we previously used. CO_2 gas standards with xCO_2 values of 953×10^{-6}, 2.19×10^{-3} and 4.96×10^{-3} were applied for calibration in order to better fit the wide range of pCO_2 in the study area. The overall uncertainty of the contents of these standards is <1%, representing the maximum errors during high pCO_2 measurement and data processing (see details in Zhai et al., 2005).

2.3.3. DIC, TAlk, nutrients, Ca and Winkler DO

DIC was determined within 24 h upon sampling by acid extraction and infrared detection, as described in Cai et al. (2004). TAlk was determined by acidimetric titration using a Gran procedure. Reference materials from Dickson's lab (CRM Batch 60#) were used to calibrate the system at a precision of ±2 μmol kg^{-1} for DIC and TAlk determinations (Cai et al., 2004).

Nutrient samples were filtered with 0.45 μm cellulose acetate filters and measured immediately onboard using a flow injection analyzer (Cai et al., 2004), among which nitrate (NO_3^-) plus nitrite (NO_2^-) were measured after reducing NO_3^- to NO_2^- with an on-line Cd coil. Ammonia (NH_4^+) was determined using the indophenol blue (IPB) spectrophotometric method after Pai et al. (2001). Ca^{2+} samples were also filtered and then acidified with concentrated nitric acid for storage. Samples were run using the classic EDTA titration method. DO concentrations in discrete samples were determined within 8 h using the classic Winkler method.

2.3.4. Bulk oxygen consumption rate incubation

Unfiltered water from Sta. 1 was incubated on-deck in a 20 L LDPE cubitainer (Fisher Scientific) with a poisoned sample as a control (see details in Zhai et al., 2005). Since the experiment was set to examine the oxygen consumption rate, our incubation was conducted under dark conditions. Subsamples were taken every 8 h. Based on the assumption that DO can be consumed along the pseudo first order reaction kinetics (see the differential equation as Eq. (1)), the pseudo first order reaction quotient was estimated using DO data collected during the incubation along the integral equation (Eq. (2)).

$$\text{Differential equation: } -\frac{d[O_2]}{dt} = k\cdot[M]\cdot[O_2] = k'\cdot[O_2] \quad (1)$$

$$\text{Integral equation: } \ln[O_2] = -k'\cdot t + A \quad (2)$$

where $[O_2]$ is the DO concentration; $[M]$ is the total concentration of oxygen consuming materials; t is incubation time; k is the integrated reaction quotient for all oxygen consumption reactions; k' is the pseudo first order reaction quotient based on the assumption of constant concentration of oxygen consuming materials; and A is a random constant. The in situ bulk oxygen consumption rate was then estimated using the pseudo first order reaction quotient and in situ DO concentrations based on Eq. (1).

3. Results

3.1. Hydrographic settings

Feb 2004 was a very dry season throughout the Pearl River basin. As a result, seawater intrusion was much farther upstream than is typical. Estuarine mix-

ing with saltwater was observable at 50 km upstream of Humen, in the suburb of Guangzhou, where salinity (S) was still ~1.0 at the low tide during our upstream survey (Fig. 2).

The water column was well mixed at Sta. 3 (typical for upstream stations) but slightly stratified in the vicinity of Humen (Fig. 3), suggesting that the salt wedge reached 30 km upstream of Humen during the survey, which is consistent with what is revealed by the surface salt front (Fig. 2).

3.2. DO distributions

Surface DO decreased upstream from >150 μmol O_2 kg^{-1} at the vicinity of the Humen Outlet down to 12–68 μmol O_2 kg^{-1} at a low salinity area (S <4). During the low tide period, this sub-oxic zone extended >20 km in part of the water channel (Fig. 2). It is noteworthy that during our upstream survey (neap tide), surface wind was moderate, especially in the upstream channel (37–50 km), where the wind speed was only ~1 m s^{-1} (Fig. 2a). This area was the most oxygen depleted, where surface DO remained at a level of <30 μmol O_2 kg^{-1} for ~13 km (Fig. 2b). When the downstream survey started during a higher tide, wind speed increased to ~3 m s^{-1} (Fig. 2b), and DO increased correspondingly. This may be due to the enhanced air injection into the water as well as tidal mixing with the more oxygenated saline water during the higher tide.

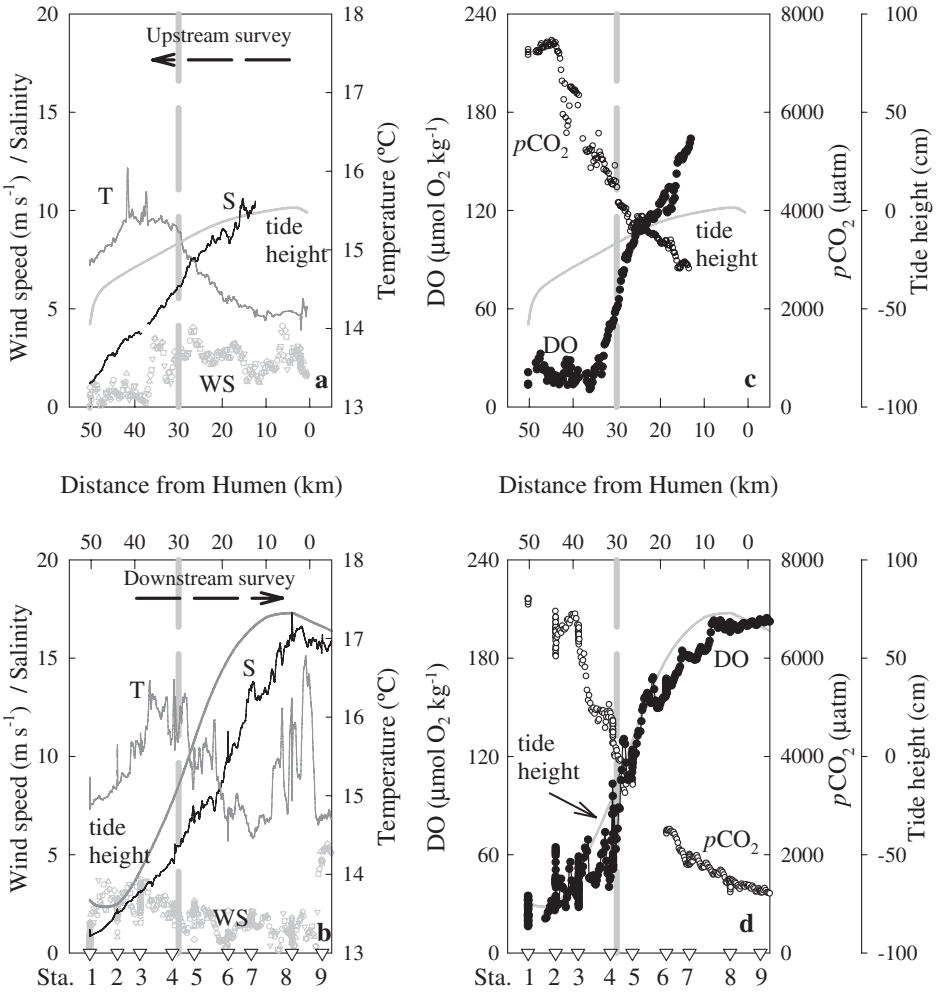

Fig. 2. Spatial distribution of surface temperature, salinity, DO, pCO_2 and wind speed in the upper reach of the Pearl River estuary. (a) Surface temperature, salinity and wind speed during the upstream survey; (b) surface temperature, salinity and wind speed during the downstream survey; (c) surface DO and pCO_2 during the upstream survey; (d) surface DO and pCO_2 during the downstream survey. Tidal heights are based on tidal cycles at an upstream station (23°06′N, 113°28′E) according to the China National Marine Data and Information Service (2004). Dashed vertical lines show ~30 km upstream of Humen, where surface DO reached ~60 μmol O_2 kg^{-1} during both the upstream and downstream surveys.

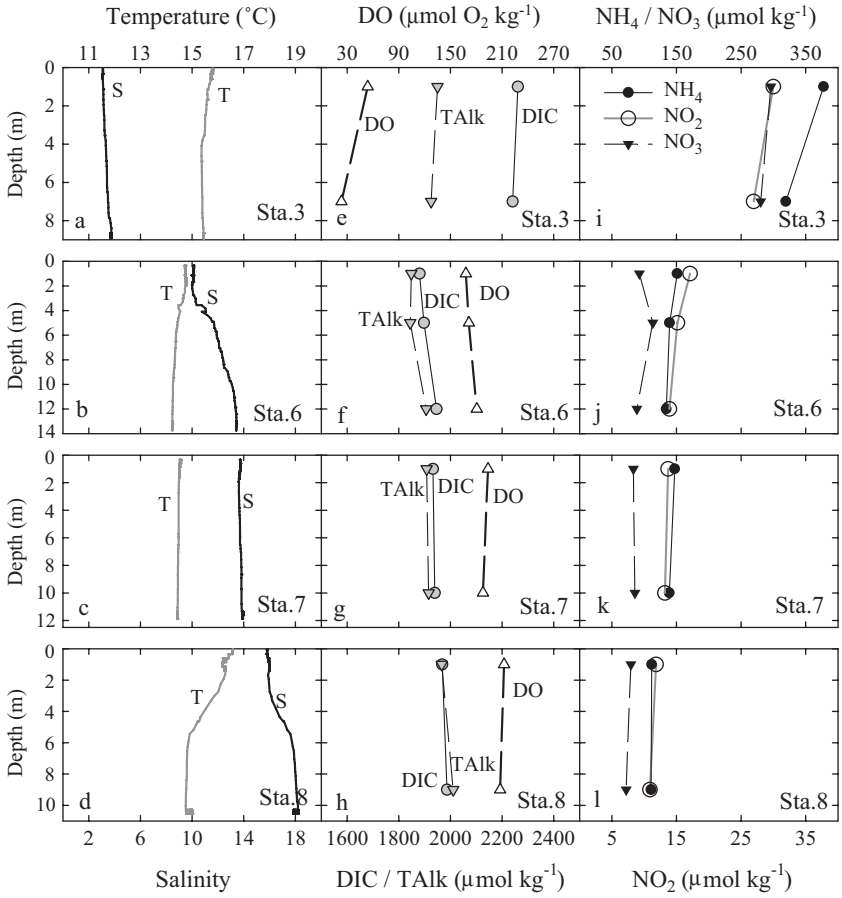

Fig. 3. Vertical profiles of temperature, salinity (a, b, c, d), DO, DIC, total alkalinity (e, f, g, h) and dissolved inorganic nitrogen (DIN) species (i, j, k, l) at selected stations upstream of Humen.

Selected DO profiles (during a flood tide) are presented in Fig. 3. DO was overall well mixed from Sta. 6 down to Humen, suggesting DO depletion in the whole water column. However, at Sta. 3 (water depth ~9 m), DO at 7 m was even lower than at the surface, reaching <30 μmol O_2 kg^{-1}. Similarly, bottom DO was ~15 μmol O_2 kg^{-1}, as compared with ~22 μmol O_2 kg^{-1} in the surface at Sta. 1 (water depth ~5 m) based on a YSI cast.

DO depletion has been observed during our previous cruises for spring and summer at the upstream of the Humen Outlet of the Pearl River estuary (Zhai et al., 2005). Further summarized in Table 2 are DO concentrations of surface waters in the upper reach of the estuary during all the seasons. Further upstream of the channel in Guangzhou, Luo (2002) also documented persistent hypoxia caused by organic pollution and nitrification. Similarly, very low DO has been also reported elsewhere in a highly polluted European estuary (upper Scheldt estuary) (Frankignoulle et al., 1996; Frankignoulle et al., 1998; Abril et al., 2000), where the low DO was attributed to the respiration of organic matter and the long residence time of freshwater in the estuarine region (Frankignoulle et al., 1996; Hellings et al., 2001).

3.3. Carbonate system

Not surprisingly and as observed previously (Zhai et al., 2005), pCO_2 mirrored DO, changing from <2000 μatm at Humen up to a very high value near the most sub-oxic zone, reaching 7000–7460 μatm (S <3.3) during the upstream survey (Fig. 2c). DIC and TAlk were distributed coherently and showed non-conservative behavior during the upper estuarine mixing (Fig. 4c). They sharply declined with salinity from 2740 μmol kg^{-1} (DIC) and 2440 μmol kg^{-1} (TAlk) at S ~1.2 down to their minima (1900 μmol kg^{-1} for DIC and 1720 μmol kg^{-1} for TAlk) at S ~5–6. At S ~6–17, DIC and TAlk progressively increased with salinity. Calcu-

Table 2
Dissolved oxygen in the surface water of the Pearl River estuary

Survey time	Location	DO (μmol O_2 kg^{-1})	Salinity	Reference
Jul 2000	Humen vicinity	96–176	0.1–1.8	Zhai et al. (2005)
May 2001	Humen vicinity	31–190	0.1–0.6	Zhai et al. (2005)
Nov 2002	Humen upstream	15–62	0.16–0.3	Dai et al., unpublished data
Feb 2004	Humen upstream	12–68	1.0–4.0	This study

lated carbonate alkalinity (CAlk) accounted for most of TAlk (Fig. 4c). At S ~1–10, the calculated CO_3^{2-} remained 5–10 μmol kg^{-1} (Fig. 4c), which was much lower than the free CO_2 of ~300 μmol kg^{-1} (Fig. 4b, c).

Surface pH increased with salinity and DO in the brackish waters ($5<S<17$) (Fig. 4a, b). At S <3, pH decreased with salinity and a minimum (~6.98) occurred at S ~3–5 (Fig. 4b). $CaCO_3$ in surface water was undersaturated throughout the study area upstream to Humen (Fig. 4d). The lowest $CaCO_3$ saturation degree (20–40%) was located within salinity ~4–6.

3.4. Inorganic nitrogen system

The concentrations of the three species of dissolved inorganic nitrogen in the surface waters especially in the low salinity region (Fig. 4), were much higher than reported for a flood season by Cai et al. (2004) or for large Chinese Rivers including the Pearl River (Zhang, 1996). The maximum concentration of NH_4^+ was >600 μmol kg^{-1} at S ~3–4 during our upstream survey (Fig. 4e). This magnitude of NH_4^+ was two times higher than NO_3^- and an order of magnitude higher than NO_2^- at the low salinity zone. The domination of NH_4^+ over other species of inorganic nitrogen was seen throughout the area under study. Overall, the concentrations of NH_4^+, NO_3^- and NO_2^- declined with salinity while NO_3^- dramatically increased during the upper estuarine mixing at S ~1–3. The maximum of NO_3^- is seen at the pH minimum (Fig. 4).

According to Guangzhou Environmental Monitoring Center, the average concentration of NH_4^+ in the Guangzhou reach of the Pearl River was ~540 μmol kg^{-1} in the first 5 months of 2004 (http://www.gemc.gov.cn). Such a high concentration of NH_4^+ clearly indicates an increasingly serious and alarming environmental problem in the upper Pearl River estuary. High levels of inorganic nitrogen have been indeed observed in the hypoxic area of the polluted Scheldt Basin (Abril and Frankignoulle, 2001) and the Seine Basins (Garnier et al., 2001). For example, >400 μmol kg^{-1} of NH_4^+ (S ~1) was documented in the upstream of the Scheldt estuary (De Bie et al., 2002).

3.5. Bulk oxygen consumption rate

Our incubation experiment showed, in the absence of light, that DO in the non-poisoned sample decreased remarkably and linearly when the incubation progressed, reaching 69 μmol O_2 L^{-1} at the end of a 38-h experiment, while DO in the control (poisoned) remained constant at ~212 μmol O_2 L^{-1} throughout the incubation period (Fig. 5). The logarithm of DO in the incubated non-poisoned sample decreased linearly with time, indicating pronounced oxygen consumption via a pseudo first order reaction. The coefficient of the pseudo first order reaction was -0.030 h^{-1} (Fig. 5). Therefore the in situ oxygen consumption rate at DO ~30 μmol O_2 kg^{-1} was ~22.5 mmol O_2 m^{-3} d^{-1}.

4. Discussion

4.1. DO consumption vs respiration

Aerobic respiration consumes dissolved oxygen and produces CO_2. As we have shown previously in Zhai et al. (2005), aerobic respiration may be a process dominating the organic matter degradation and DO consumption in the Pearl River estuary in spring and summer.

In the study area, at S ~1–10, CO_3^{2-} remained 5–10 μmol kg^{-1}, which equals to 1.5–12% of the free CO_2 (see Fig. 4b and c). Meanwhile, there does not seem to be non-carbonate alkaline matter (e.g. ammoniac alkalinity is negligible as compared with carbonate alkalinity although the ammonia is very high) at pH ~7 to titrate the free CO_2 in water. Therefore it is valid to directly link aqueous free CO_2 with DO consumption using a stoichiometric approach as we did previously (Zhai et al., 2005).

Based on Fig. 6, the excess CO_2 is linearly correlated with oxygen depletion at S ~4–10 with a ΔCO_2: $(-\Delta O_2)$ ratio of 0.73. This is within the ranges of Redfield respiration (see Zhai et al., 2005), suggesting strong aerobic respiration domination. The departure from the Redfield respiration at S ~1–4 may thus imply additional CO_2 production processes other than aerobic respiration.

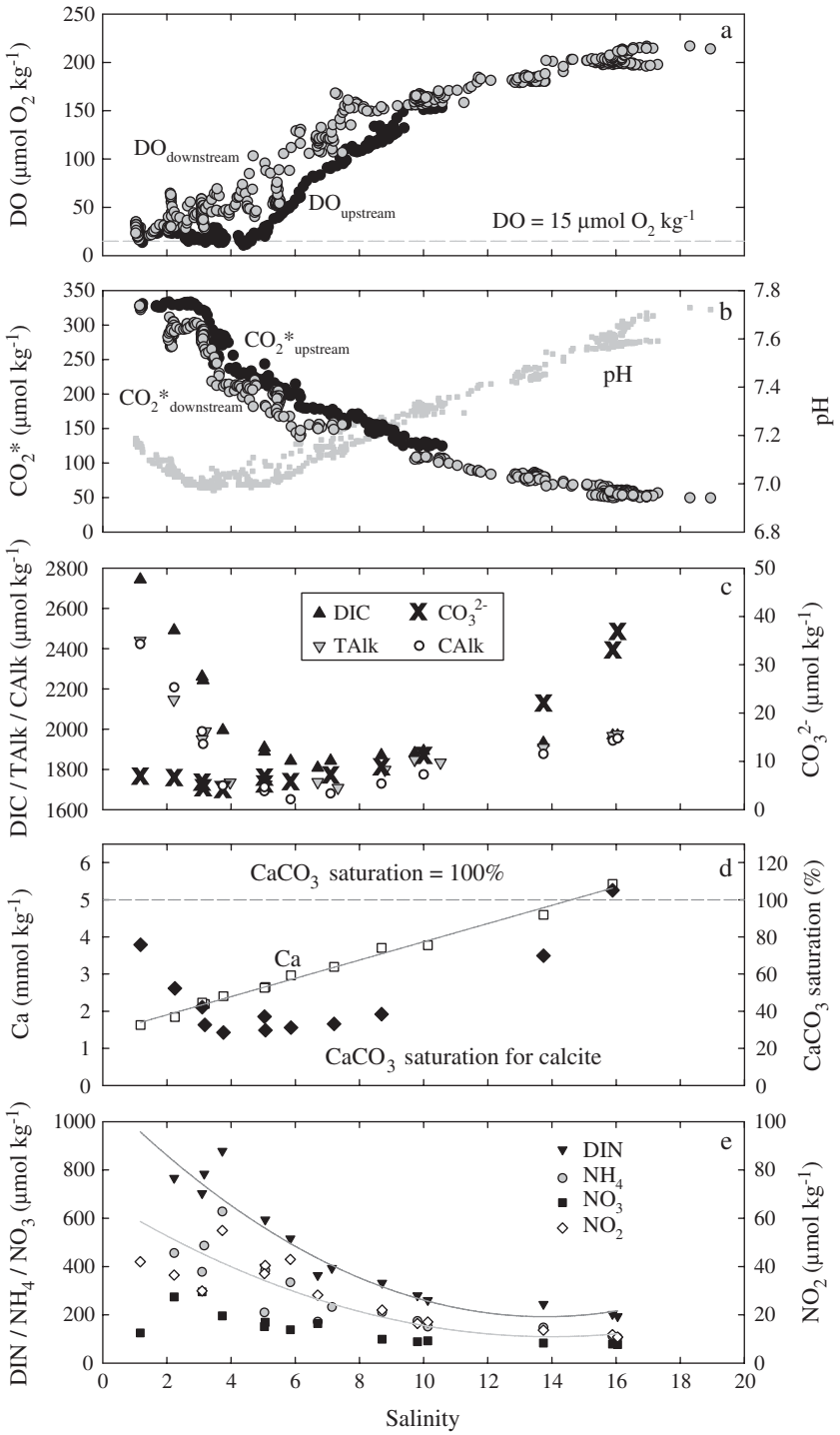

Fig. 4. Mixing processes of DO (a), carbonate system (b and c), calcium (d) and dissolved inorganic nitrogen species (e) in surface waters of the upper reach of the Pearl River estuary. The carbonate alkalinity (CAlk) and CO_3^{2-} were computed based on combination of pCO_2 and discrete DIC data. pH data shown here were also calibrated against pH computed based on combination of pCO_2 and discrete DIC data. Dickson and Millero (1987) constants were used for the carbonate system calculation. The $CaCO_3$ solubility was computed according to Mucci (1983). Dashed line in the panel (d) represents 100% saturation degree of $CaCO_3$ (Calcite).

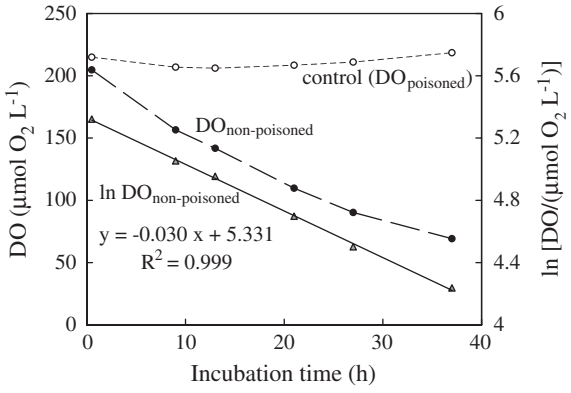

Fig. 5. DO evolution during a pelagic respiration/bulk oxygen consumption rate incubation. Initial sample was taken from Sta. 1.

The on-deck incubation gave a surprisingly high pseudo first order oxygen consuming reaction quotient as $-0.030\ h^{-1}$ (Fig. 5), as compared with $-0.012\ h^{-1}$ obtained in spring of 2001 (Zhai et al., unpubilished data). According to Eq. (1), the pseudo first order reaction quotient is in direct proportion to the total concentration of oxygen consuming materials. This enhancement of bulk oxygen consumption observed in the present study thus may have an implication of additional processes over the aerobic respiration although we are aware that there may be significant difference in types of organic matter between the two seasons.

4.2. Nitrification

Since $CaCO_3$ was overall undersaturated in the area (Fig. 4d), calcification should be excluded as a major CO_2 production process. Then nitrification should be considered as a potential major process that controls the development of the oxygen depletion and CO_2 production.

Nitrification typically contains ammonia oxidation (Eq. (3)) and nitrite oxidation (Eq. (4)) (US EPA, 1993):

$$NH_3 + \frac{3}{2}O_2 \rightarrow NO_2^- + H^+ + H_2O \quad (3)$$

$$NO_2^- + \frac{1}{2}O_2 \rightarrow NO_3^-. \quad (4)$$

Coupling the two oxidation processes and assimilation reactions, the overall reaction describing the complete nitrification process should be (modified from US EPA, 1993):

$$NH_4^+ + 1.89O_2 + 1.98HCO_3^- \rightarrow 0.984NO_3^- + 0.016C_5H_7O_2N + 1.90CO_2 + 2.93H_2O. \quad (5)$$

Note that $C_5H_7O_2N$ is the empirical cell stoichiometry for bacteria when phosphorus is excluded. Eq. (5) represents an oversimplification of the nitrification process and is only valid for an environment with neutral pH and abundant HCO_3^-, such as the area under study (see Results). Under these conditions, in addition to the consumption of DO and bicarbonate alkalinity, nitrification should produce NO_3^- and free CO_2 along $\Delta NO_3/(-\Delta CAlk)$ and $\Delta CO_2/(-\Delta O_2)$ ratios of 0.984/1.98 and 1.90/1.89, respectively, to the environment (Eq. (5)). This is seen at salinities between 1 and 4 with an approximate $\Delta CO_2/(-\Delta O_2)$ ratio of 1.0 (Fig. 6). Note that scattered data are also observable, overlapping the Redfield respiration ranges (Fig 6), and thus the validation of the Redfield stoichiometry to diagnose nitrification needs further investigations.

More significantly, the curvature of the NH_4^+ plot (concave downward in $NH_4^+ - S$ plot) suggests NH_4^+ removal during mixing, most likely via nitrification (Fig. 4e). This is particularly clear in the zone of S ~1–7. The nitrification mechanism is consistent with a local NO_3^- peak (Fig. 4e) and a pH minimum (Fig. 4b) within this salinity zone. High and nearly constant NO_2^- (30–50 μmol kg^{-1}) in the upstream waters with S ~1–6

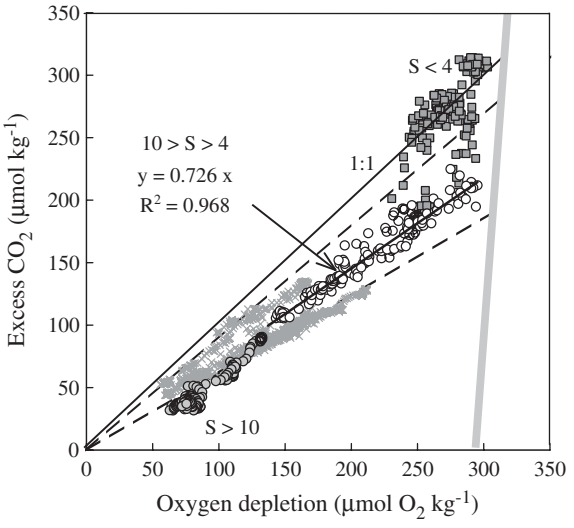

Fig. 6. Excess CO_2 vs. surface oxygen depletion upstream Humen, on Feb 14, 2004. Note that excess $CO_2 = CO_2^* - K_H^{CO2} \times pCO_2$ (in air), and oxygen depletion $= [O_2]_{eq} - [O_2]$, where, $[CO_2^*]$ is the concentration of total free CO_2, (i.e., $[CO_2^*] = [CO_2] + [H_2CO_3] = K_H^{CO2} \times pCO_2$ in water); K_H^{CO2} is the solubility coefficient of CO_2; $[O_2]$ is the DO concentration at equilibrium with the atmosphere, $[O_2]$ is the in situ DO concentration. The two dashed lines show the upper limit (0.90) and the lower limit (0.62) for stoichiometric $\Delta CO_2 : (-\Delta O_2)$ ratio of aerobic respiration in the environment with abundance of HCO_3^- (See Zhai et al., 2005). Grey x symbols represent data from our previous spring and summer surveys at the vicinity of the Humen Outlet from Zhai et al. (2005).

(Fig. 4e) also lends evidence for active and approximately balanced nitrification between ammonia oxidation and nitrate production in the water column.

Moreover, the NH_4^+–S plot (Fig. 4e) has a curvilinear regression of: $NH_4^+ = 0.0065S^3 + 2.96S^2 - 85.15S + 681.94$ ($R^2 = 0.81$). Therefore, $d(NH_4^+)/dS = 0.018S^2 + 5.92S - 85.15$. At $S = 2$–5, the dilution corrected NH_4^+ change, i.e., $\Delta(S \times dC/dS)$ is -153 μmol kg^{-1}. Oxidation of this amount of NH_4^+ to NO_3^- requires 289 μmol O_2 kg^{-1} based on Eq. (5) and results in a 306 μmol kg^{-1} decrease in TAlk. Note that DO depletion at $S < 5$ during our upstream survey was 280–300 μmol O_2 kg^{-1}, which is consistent with the oxygen demand of the nitrification. At the same time, saturated DO upstream of Sta. 4 would be 300–317 μmol O_2 kg^{-1}. Thus it is clear that most consumption was caused by NH_4^+ oxidation.

Luo (2002) indeed reported very strong nitrification in a channel of the Pearl River flowing through Guangzhou based upon an incubation experiment which showed that BOD (biological oxygen demand) was significantly inhibited in samples with the addition of a nitrifying inhibitor. In a parallel investigation which was conducted 2 months after our cruise (April 2004) in the same region as the present study, Xu et al. (2005) also revealed a very high nitrification rate using sediment samples collected at a station 4–5 km upstream to our Sta. 1, suggesting very high DO demand during the ammonia oxidation processes.

Finally, in a recent cruise in Jan 2005 under a similar hydrological condition to the present study, we measured the water column nitrification rate at both a station within the Guangzhou section and a station close to Sta. 1, where high nitrification rates, measured via a nitrite evolution method, were 4.8 and 5.8 mmol N m^{-3} d^{-1}, respectively, (Dai et al., unpublished data). Taken together, nitrification is indeed significant in the region under study, which substantially contributes to the CO_2 production and DO consumption.

It is worth noting that nitrification is usually coupled with denitrification under low DO conditions whereby oxidation of NH_4^+ generates a source of nitrate for denitrifying bacteria (e.g., Wang et al., 2003). The nitrification coupled with denitrification leads to losses of nitrogen to the atmosphere as nitrious oxide and/or nitrogen gas (Herbert, 1999). In our study area, the concave downward shape in the plot of DIN (sum of inorganic nitrogen species, Fig. 4e) against salinity suggests that denitrification also occurred. This is also supported by Xu et al. (2005) who obtained an extremely high concentration of nitrous oxide. Its saturation degree ranged from 674% to 4134%. However, denitrification was not the focus of this study and thus will not be further discussed.

5. Concluding remarks

As early as in the 1990s, >400 μmol kg^{-1} of NH_4^+ (S ~1) was documented in the upstream of the Scheldt estuary (Frankignoulle et al., 1996; De Bie et al., 2002). The situation of the upstream Pearl River estuary under this study (>300 μmol kg^{-1} of NH_4^+ at $S < 5$) is similar in many ways to the Scheldt estuary in the 1990s.

Our results are site specific and may be limited to a very dry season, but have much broader implications regarding environmental deterioration associated with sewage discharge. Our results have clearly demonstrated the linkage between the sewage discharge, organic degradation, nitrification and oxygen depletion. Garnier et al. (2001) have pointed out based upon their observations in the Seine River Estuary that summer oxygen depletion is a constant feature of the ecological functioning of the system and nitrification was a major controlling processes, probably typical of large river systems strongly impacted by domestic and industrial effluents, which lack the treatment through a nitrification step, as is still often the case in Europe. Such oxygen depletion is now also happening in Asia and many lessons can be learned from the environment deterioration evolution in Europe.

This study also demonstrated the close linkage between DO consumption and the carbonate system, i.e. a coupling between nitrogen and carbon cycling. Analysis based on the Redfield stoichiometry is a useful approach in attempting to diagnose the processes contributing to surface hypoxia.

Acknowledgements

This research was supported by the Natural Science Foundation of China through grants #90211020, #40490260, #40228007 and #40406023, and by the Hi-Tech Research and Development Program of China (#2002AA635140). We thank Zhaozhang Chen for assistance with CTD data collection and processing, and Baoshan Chen for Ca measurements. Wuqi Ruan and Fan Zhang along with the crew of Yanping II provided much help during the sampling cruises. Reviews and/or comments from Rodney T. Powell and three anonymous reviewers greatly improved the quality of the paper.

References

Abril, G., Riou, S.A., Etcheber, H., Frankignoulle, M., Wit, R. de, Middelburg, J.J., 2000. Transient, tidal time-scale, nitrogen trans-

formations in an estuarine turbidity maximum-fluid mud system (the Gironde, south-west France). Estuarine, Coastal and Shelf Science 50, 703–715.

Abril, G., Frankignoulle, M., 2001. Nitrogen-alkalinity interactions in the highly polluted Scheldt basin (Belgium). Water Research 35, 844–850.

Abril, G., Etcheber, H., Delille, B., Frankignolle, M., Borges, A.V., 2003. Carbonate dissolution in the turbid and eutrophic Loire estuary. Marine Ecology Progress Series 259, 129–138.

Balls, P.W., Brockie, N., Dobson, J., Johnston, W., 1996. Dissolved oxygen and nitrification in the upper Forth estuary during summer (1982–1992): patterns and trends. Estuarine, Coastal and Shelf Science 42, 117–134.

Borsuk, M.E., Stow, C.A., Luettich, R.A., Paerl, J.H.W., Pinckney, J.L., 2001. Modeling oxygen dynamics in an intermittently stratified estuary: estimation of process rate using field data. Estuarine, Coastal and Shelf Science 52, 33–49.

Cai, W.-J., Dai, M., Wang, Y., Zhai, W., Huang, T., Chen, S., Zhang, F., Chen, Z., Wang, Z., 2004. The biogeochemistry of inorganic carbon and nutrients in the Pearl River estuary and the adjacent Northern South China Sea. Continental Shelf Research 24, 1301–1319.

Cheng, Z., 2001. Decadal variation of hydrological status in stream network area and the eight outlets of Pearl River estuary delta. Acta Scientiarum Naturalium Universitatis Sunyatseni 40, 29–31 (in Chinese).

De Bie, M.J.M., Middelburg, J.J., Starink, M., Laanbroek, H.J., 2002. Factors controlling nitrous oxide at the microbial community and estuarine scale. Marine Ecology Progress Series 240, 1–9.

Dickson, A.G., Millero, F.J., 1987. A comparison of the equilibrium constants for the dissociation of carbonic acid in the seawater media. Deep-Sea Research I 34, 1733–1743.

Engle, V.D., Summers, J.K., Macauley, J.M., 1999. Dissolved oxygen conditions in northern Gulf of Mexico estuaries. Environmental Monitoring and Assessment 57, 1–20.

Frankignoulle, M., Borge, I., Wollast, R., 1996. Atmospheric CO_2 fluxes in a highly polluted estuary (the Scheldt). Limnology and Oceanography 41, 365–369.

Frankignoulle, M., Abril, G., Borges, A., Bourge, I., Canon, C., DeLille, B., Libert, E., Theate, J.M., 1998. Carbon dioxide emission from European estuaries. Science 282, 434–436.

Garnier, J., Servais, P., Billen, G., Akopian, M., Brion, N., 2001. The oxygen budget in the Seine estuary: balance between photosynthesis and degradation of organic matter. Estuaries 24, 964–977.

Guangzhou Chorography Compilation Committee, 1998. Natural Geography Record. Guangzhou Publishing House, Guangzhou. http://www.gzsdfz.org.cn.

Hellings, L., Dehairs, F., Van Damme, S., Baeyens, W., 2001. Dissolved inorganic carbon in the highly polluted estuary (the Scheldt). Limnology and Oceanography 46, 1406–1414.

Herbert, R.A., 1999. Nitrogen cycling in coastal marine ecosystems. Fems Microbiology Reviews 23, 563–590.

Ho, K.C., Hui, K.C.C., 2001. Chemical contamination of the East River (Dongjiang) and its implication on sustainable development in the Pearl River Delta. Environment International 26, 303–308.

Huang, X.P., Huang, L.M., Yue, W.Z., 2003. The characteristics of nutrients and eutrophication in the Pearl River estuary, South China. Marine Pollution Bulletin 47, 30–36.

Kemp, W.M., Sampou, P.A., Garber, J., Tuttle, J., Boynton, W.R., 1992. Seasonal depletion of oxygen from bottom waters of Chesapeake Bay: roles of benthic and planktonic respiration and physical exchange processes. Marine Ecology Progress Series 85, 137–152.

Lawrence, P., Sanford, K., Sellner, G., Breitburg, D.L., 1990. Covariability of dissolved oxygen with physical processes in the summertime Chesapeake Bay. Journal of Marine System 48, 567–590.

Li, D.J., Zhang, J., Huang, D.J., Wu, Y., Liang, J., 2002. Oxygen depletion off the Changjiang (Yangtze River) Estuary. Science in China Series D-Earth Sciences 45, 1137–1146.

Luo, J.-H., 2002. The analysis of the primary cause of the low dissolved oxygen of the partial water body in the Guangzhou reach of the Pearl River. Research of Environmental Sciences 15, 8–11 (in Chinese).

Mucci, A., 1983. The solubility of calcite and aragonite in seawater at various salinities, temperatures, and one atmosphere total pressure. American Journal of Science 283, 780–799.

Pai, S.-C., Y.-j., T., Yang, T.-I., 2001. pH and buffering capacity problems involved in the determination of ammonia in saline water using the indophenol blue spectrophotometric method. Analytica Chimica Acta 434, 209–216.

PRWRC/PRRCC, 1991. The Pearl River Records (Zhujiang Zhi). Guangdong Science and Technology Press, Guangzhou, pp. 162–165 (in Chinese).

Rabalais, N.N., Turner, R.E., 2001. Hypoxia in the northern gulf of Mexico: description, causes and consequences. In: Rabalais, N.N., Turner, R.E. (Eds.), Coastal Hypoxia: consequences for living resources and ecosystems. American Geophysical Union, Washington D.C., pp. 1–36.

Rabalais, N.N., Turner, R.E., Wiseman, W.J., 2002. Gulf of Mexico hypoxia, aka "The dead zone". Annual Review of Ecology and Systematics 33, 235–263.

Ritter, C., Montagna, P.A., 1999. Seasonal hypoxia and models of benthic response in a Texas Bay. Estuaries 22, 7–20.

Tao, Y.X., Hills, P., 1999. Assessment of alterative wastewater treatment approaches in Guangzghou, China. Water Science and Technology 39, 227–234.

US EPA, 1993. Process design manual for nitrogen removal. EPA/625/R-93/010, U.S. Environmental Protection Agency, Washington, DC. 88pp.

Wang, F., Juniper, S.K., Pelegri, S.P., Macko, S.A., 2003. Denitrification in sediments of the Laurentian Trough, St. Lawrence Estuary, Quebec, Canada. Estuarine, Coastal and Shelf Science 57, 515–522.

Xu, J., Wang, Y., Yin, J., Wang, Q., Zhang, F., He, L., Sun, C., 2005. Transformation of dissolved inorganic nitrogen species and nitrification and denitrification processes in the near sea section of Zhujiang River. Acta Scientiae Circumstantiae 25, 686–692 (in Chinese).

Zhai, W., Dai, M., Cai, W.-J., Wang, Y., Wang, Z., 2005. High partial pressure of CO_2 and its maintaining mechanism in a subtropical estuary, the Pearl River estuary, China. Marine Chemistry 93, 21–32.

Zhang, J., 1996. Nutrient elements in large Chinese estuaries. Continental Shelf Research 16, 1023–1045.

Zhang, Q., Qian, D., He, K., 1999. Dissolved oxygen in the vicinity of Guangzhou of the Pearl River. Guangzhou Center for Environmental Monitoring (http://www.gemc.gov.cn/xueshu/lunwen99/9.htm).

Zhao, H., 1990. Evolution of the Pearl River Estuary. Ocean Press, Beijing. 357 pp. (in Chinese).